The 2004 European Signal Processing Conference
Vienna, September 7–10, 2004, http://www.nt.tuwien.ac.at/eusipco2004/

BEAM DESIGN FOR A PING-PONG-SAMPLED LINEAR RECEIVE ARRAY

Jeffrey O. Coleman http://alum.mit.edu/www/jeffc
Dan P. Scholnik dan.scholnik@nrl.navy.mil

Naval Research Laboratory (http://www.nrl.navy.mil/)
Radar Division, Signal Processing Theory & Methods Section

ABSTRACT

Aliasing of far-field plane-wave information is avoided using only half the conventional Nyquist sample rate when sample timing is staggered on adjacent elements of a linear antenna array. The receive version of the array is examined here. The required upsampling beamformer structure is presented, and examples illustrate the pattern-design process.

1 INTRODUCTION

Processing of signals from receive array antennas has long been viewed as a sort of spatial sampling of the electromagnetic field. More recently, the advent of DSP-based receivers has introduced sampling in time into the system as well. This historical process naturally led to the sampling issues being worked out separately in time and in space. Recently it was shown, however, that it is beneficial to consider the sampling jointly in spacetime [1]. Specifically, for a linear antenna array the mapping between plane waves in the far field and the array output remains free of aliasing when individual element outputs are sampled at only half the usual Nyquist sample rate of twice the one-sided signal bandwidth, provided that sample times are staggered for alternate elements.

Our earlier paper [1] explored this sampling scheme in a general way but did not consider specific applications in detail. Here we consider a receive array in particular and examine the DSP realization of a wideband beam from IF samples. Wideband beam synthesis for such a system digitally filters the individual element outputs before summing. These filters, taken jointly as a single system, turn out to have an antialiasing role as well as the usual role of determining the shape of the beam and its sidelobes versus frequency. We focus on the design of this filtering using optimization methods largely developed earlier [2, 3, 4] but tailored here to this specific application. We go only as far as coefficient design, as DSP-hardware issues are the same as for any other high-speed DSP system. Space constraints here limit the depth of the mathematical presentation, but a thorough mathematical development will follow in a subsequent paper.

This work was supported by base funding at the Naval Research Laboratory.

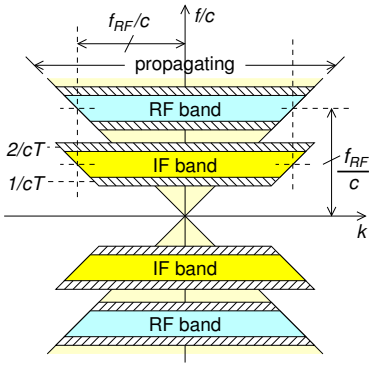

Figure 1: Incident far-field plane waves drive a line array in Helmholz cone $|f|/c \geq |k|$, where k is spatial frequency along the array. The RF band from each element is shifted to IF to vertically center filter transition bands (hatched) on the edges of a Nyquist zone for later sampling.

2 THEORY

The first section below introduces ping-pong sampling in a way that is somewhat specific to the receive-array case. We hope that it will serve as a gentler introduction than the original paper [1], which it overlaps somewhat. Section 2.2 on the beam synthesizer is new material, not before presented.

2.1 Ping-Pong Sampling

Let us begin by establishing what we are sampling. Given unit vector $\widehat{u}$, the output of an antenna element at $\mathbf{x} = x\widehat{u}$ and that output's 2D Fourier transform are functions of $\boldsymbol{t} \triangleq \left[\begin{smallmatrix} x \\ ct \end{smallmatrix}\right]$ and $\boldsymbol{f} \triangleq \left[\begin{smallmatrix} k \\ f/c \end{smallmatrix}\right]$ respectively, and that transform takes the form

$$\mathrm{L}\left(\left[\begin{smallmatrix} k \\ f/c \end{smallmatrix}\right]\right) \triangleq \int \vec{\mathbf{E}}\left(\left[\begin{smallmatrix} k\widehat{u}+\mathbf{k}_\perp \\ f/c \end{smallmatrix}\right]\right) \cdot \vec{\boldsymbol{\Phi}}\left(\left[\begin{smallmatrix} k\widehat{u}+\mathbf{k}_\perp \\ f/c \end{smallmatrix}\right]\right) d\mathbf{k}_\perp. \quad (1)$$

where Fourier pair $\vec{\mathbf{e}}(\mathbf{t}) \leftrightarrow \vec{\mathbf{E}}(\mathbf{f})$ is the electric field versus 4D spacetime arguments $\mathbf{t} \triangleq \left[\begin{smallmatrix} \mathbf{x} \\ ct \end{smallmatrix}\right]$ and $\mathbf{f} \triangleq \left[\begin{smallmatrix} \mathbf{k} \\ f/c \end{smallmatrix}\right]$ and where $d\mathbf{k}_\perp$ denotes differential area in the plane normal to $\widehat{u}$. For any given f, this integral combines incoming signals with directions of arrival at the same angle with $\widehat{u}$ and applies element pattern $\vec{\boldsymbol{\Phi}}(\mathbf{f})$. A conjugate pair of Fourier field components at $\pm\left[\begin{smallmatrix} \mathbf{k} \\ f/c \end{smallmatrix}\right]$ forms a plane wave propagating in the $-\mathbf{k}$ direction at a speed given by the *Helmholz relation* to be $|f|/\|\mathbf{k}\| = c$, which here becomes $|f| = c\,\|\,k\widehat{u}+\mathbf{k}_\perp\| \geq c|k|$ and so, if only far-field sources are present, restricts the $\boldsymbol{f} = \left[\begin{smallmatrix} k \\ f/c \end{smallmatrix}\right]$ values of Fourier components in $\mathrm{L}\left(\left[\begin{smallmatrix} k \\ f/c \end{smallmatrix}\right]\right)$ to be inside the double cone of propagating frequencies shown in Fig. 1.

At this element output let an RF band centered at f_{RF} then be translated up or down in frequency as sketched in

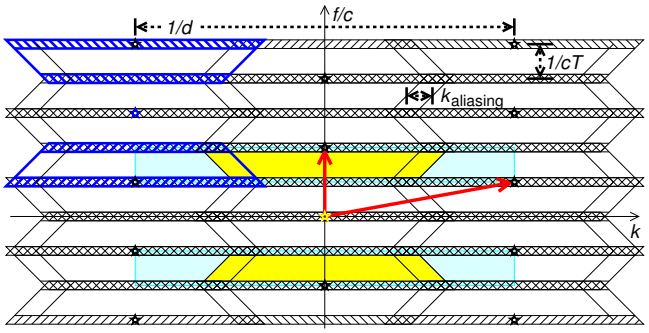

Figure 2: Ping-pong sampling the IF band of Fig. 1 creates spectral replicas—one is shown in bold—with the origin mapped to the points (stars) in the spectral-replication lattice $\boldsymbol{\Delta f}\,\mathbb{Z}^2$. The heavy arrows denote suitable lattice basis vectors. Aliasing in the vertical zig-zag regions is controlled by setting d. The two shaded boxes of width-$\frac{1}{d}$ together form one period of the beam-synthesizer filter's frequency response. (Closeup in Fig. 5.)

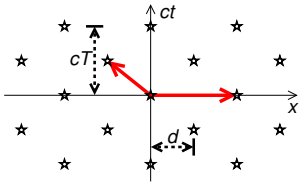

Figure 3: Sampling times $\{ct\}$ of signals from elements at displacements $\{x\}$ along a line array. The basis vectors of sample-location lattice $\mathbf{T}\mathbb{Z}^2$ are shown as heavy arrows.

Fig. 1, with the transition bands created by bandlimiting filters centered on successive integral multiples of $\frac{1}{cT}$ at IF, where scalar T is a practical sampling interval. Let Fourier pair $\ell_{\text{IF}}(\boldsymbol{t}) \leftrightarrow \text{L}_{\text{IF}}(\boldsymbol{f})$ be the resulting IF signal. Differential

$$d\underline{\ell}(\boldsymbol{t}) = \ell_{\text{IF}}(\boldsymbol{t}) \sum_{\mathbf{n}\in\mathbb{Z}^2} \delta(\boldsymbol{t}-\mathbf{T}\mathbf{n})\, d\boldsymbol{t} = \sum_{\mathbf{n}\in\mathbb{Z}^2} \ell_{\mathbf{n}}\, \delta(\boldsymbol{t}-\mathbf{T}\mathbf{n})\, d\boldsymbol{t} \quad (2)$$

with *array sample* $\ell_{\mathbf{n}} \triangleq \ell_{\text{IF}}(\mathbf{T}\mathbf{n})$ is then our array output. The delta functions fall on a *sample-location lattice* $\mathbf{T}\mathbb{Z}^2$ comprising all integer combinations of two linearly independent basis vectors, the columns of 2×2 *sample-interval matrix* $\mathbf{T}$. Here samples are taken at a discrete but infinite set of x values, but the beam-synthesis process to be developed will use only a finite subset of these. An actual system would have a physical antenna element, an RF front end, and sampling hardware at $x\widehat{u}$ for each x value in that finite subset.

The Fourier transform of $d\underline{\ell}(\boldsymbol{t})$ is [1]

$$\text{L}(\boldsymbol{f}) \triangleq \int \text{e}^{-\text{j}2\pi \boldsymbol{f}^T \boldsymbol{t}}\, d\underline{\ell}(\boldsymbol{t}) = \sum_{\mathbf{n}\in\mathbb{Z}^2} \ell_{\mathbf{n}}\, \text{e}^{-\text{j}2\pi \boldsymbol{f}^T \mathbf{T}\mathbf{n}}$$

$$= \frac{1}{|\det(\mathbf{T})|} \sum_{\mathbf{k}\in\mathbb{Z}^2} \text{L}_{\text{IF}}(\boldsymbol{f} - \boldsymbol{\Delta f}\,\mathbf{k}). \quad (3)$$

Spectral-replication lattice $\boldsymbol{\Delta f}\,\mathbb{Z}^2$, the *dual* of sample-location lattice $\mathbf{T}\mathbb{Z}^2$, is defined by *spectral-period matrix* $\boldsymbol{\Delta f} \triangleq \mathbf{T}^{-T}$.

Conventionally, sample-interval matrix $\mathbf{T}$ and spectral-period matrix $\boldsymbol{\Delta f}$ are implicitly diagonal, making sample-location lattice $\mathbf{T}\mathbb{Z}^2$ and spectral-replication lattice $\boldsymbol{\Delta f}\,\mathbb{Z}^2$ into rectangular grids. This results, however, in inefficient packing by (3) of spectral replicas of the IF band of Fig. 1. Our alternative is the "ping pong" spectral-replication lattice shown in Fig. 2, where setting $k_{\text{aliasing}} = 0$ results in replicas

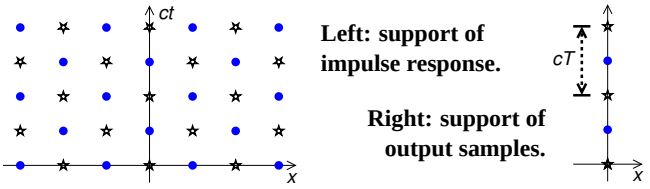

Figure 4: The beam synthesizer's input lattice $\mathbf{T}\mathbb{Z}^2$ (left, stars) and output lattice $\left[\begin{smallmatrix}0\\ cT/2\end{smallmatrix}\right]\mathbb{Z}$ (right) are both sublattices of superlattice $\mathbf{T_w}$ (left, stars and dots) on which 2D filtering is done.

tiling the plane exactly, with no aliasing and no empty spectral space. The $k_{\text{aliasing}} > 0$ cases explored in examples later are slightly less expensive due to increased element spacing.

To determine the associated sample-interval matrix $\mathbf{T}$ and spectral-period matrix $\boldsymbol{\Delta f}$, observe that spectral-replication lattice $\boldsymbol{\Delta f}\,\mathbb{Z}^2$ in Fig. 2 comprises integer combinations of the two basis vectors shown, the columns of

$$\boldsymbol{\Delta f} = \begin{bmatrix} 0 & \frac{1}{2d} \\ \frac{2}{cT} & \frac{1}{cT} \end{bmatrix}, \quad (4)$$

where

$$\frac{1}{d} = 4\frac{f_{\text{RF}}}{c} - 2k_{\text{aliasing}}. \quad (5)$$

From (4) then,

$$\mathbf{T} = \boldsymbol{\Delta f}^{-T} = \begin{bmatrix} -d & 2d \\ \frac{cT}{2} & 0 \end{bmatrix}.$$

The basis-vector columns of $\mathbf{T}$ and their integer combinations, the sample-location lattice $\mathbf{T}\mathbb{Z}^2$, are sketched in Fig. 3. At each element location x sampling times appear at intervals of T, but those times are staggered $180°$ for adjacent elements so that samples are taken of half the element outputs after every interval of $T/2$. In the special $k_{\text{aliasing}} = 0$ no-aliasing case, (5) sets element spacing d to a quarter wavelength at RF band center, closer than the conventional approach requires.

2.2 The Beam Synthesizer

The beam synthesizer's input samples $\{\ell_{\mathbf{n}}\}$ are associated by (2) with coordinates in lattice $\mathbf{T}\mathbb{Z}^2$, shown in Fig. 3, but that lattice does not contain all required output-sample locations. The width in f of the IF band in Fig. 1 requires a sampling rate of at least $2/T$ to avoid aliasing the scalar beam-synthesizer output. The required minimal set of output points then is as shown on the right in Fig. 4. They are placed at $x = 0$ for convenience. When input and output sample rates differ in ordinary 1D DSP, we filter at a higher rate that is a multiple of the input and output rates. The same idea applies here. We filter on the common superlattice $\mathbf{T_w}\mathbb{Z}^2$, where $\mathbf{T_w} \triangleq \left[\begin{smallmatrix} d & 0 \\ 0 & cT/2 \end{smallmatrix}\right]$, sketched on the left in Fig. 4 (stars and dots). Beam synthesis then comprises three steps:

1. Zero-interpolate the input onto superlattice $\mathbf{T_w}\mathbb{Z}^2$.
2. Filter the result with a 2D convolution in $\mathbf{T_w}\mathbb{Z}^2$.
3. Evaluate the output only on lattice points having $x = 0$.

Polyphase decomposition of the impulse response streamlines implementation. In Fig. 4 output samples on $\left[\begin{smallmatrix}0\\ cT\end{smallmatrix}\right]\mathbb{Z}$

(right, stars) are computed with impulse-response coefficients on lattice $\mathbf{T}\mathbb{Z}^2$ (left, stars), and output samples on offset lattice $\left[\begin{smallmatrix}0\\cT\end{smallmatrix}\right]\mathbb{Z}+\left[\begin{smallmatrix}0\\cT/2\end{smallmatrix}\right]$ (right, dots) are computed using coefficients from offset lattice $\mathbf{T}\mathbb{Z}^2+\left[\begin{smallmatrix}0\\cT/2\end{smallmatrix}\right]$ (left, dots). The three-step procedure above yields a signal with Fourier transform

$$\mathrm{B}(f) = d\int_{\frac{-1}{2d}}^{\frac{1}{2d}} \mathrm{W}\left(\left[\begin{smallmatrix}k\\f/c\end{smallmatrix}\right]\right)\mathrm{L}\left(\left[\begin{smallmatrix}k\\f/c\end{smallmatrix}\right]\right)\,dk, \tag{6}$$

where we take $\{w_{\mathbf{n}}\}$ as the filter coefficients so that

$$d\underline{w}(\boldsymbol{t}) = \sum_{\mathbf{n}\in\mathbb{Z}^2} w_{\mathbf{n}}\,\delta(\boldsymbol{t}-\mathbf{T}_{\mathbf{w}}\mathbf{n})\,d\boldsymbol{t}$$

$$\mathrm{W}(\boldsymbol{f}) = \int \mathrm{e}^{-\mathrm{j}2\pi\boldsymbol{f}^T\boldsymbol{t}}\;d\underline{w}(\boldsymbol{t}) = \sum_{\mathbf{n}\in\mathbb{Z}^2} w_{\mathbf{n}}\,\mathrm{e}^{-\mathrm{j}2\pi\boldsymbol{f}^T\mathbf{T}_{\mathbf{w}}\mathbf{n}}.$$

Each of the three beam-synthesis steps above is reflected in (6). The functions in the integrand have periodicities

$$\begin{aligned}\mathrm{L}(\boldsymbol{f}) &= \mathrm{L}(\boldsymbol{f}-\boldsymbol{f}') \qquad \text{for any } \boldsymbol{f}'\in\boldsymbol{\Delta f}\,\mathbb{Z}^2 = \mathbf{T}^{-T}\mathbb{Z}^2\\ \mathrm{W}(\boldsymbol{f}) &= \mathrm{W}(\boldsymbol{f}-\boldsymbol{f}') \qquad \text{for any } \boldsymbol{f}'\in\mathbf{T}_{\mathbf{w}}{}^{-T}\mathbb{Z}^2,\end{aligned}$$

and the lattice $\mathbf{T}_{\mathbf{w}}{}^{-T}\mathbb{Z}^2$ of spectral offsets is half as dense as spectral-replication lattice $\boldsymbol{\Delta f}\,\mathbb{Z}^2$, corresponding in the 2D spacetime domain to $\mathbf{T}_{\mathbf{w}}\mathbb{Z}^2$, the support of the filter's 2D impulse response, being twice as dense as sample-location lattice $\mathbf{T}\mathbb{Z}^2$. The zero-interpolation step does not affect the spectra used in the integral, but it corrects the factor of two difference in sample density computationally.

The second step, filtering, corresponds to the weighting of $\mathrm{L}(\boldsymbol{f})$ by $\mathrm{W}(\boldsymbol{f})$ in (6). The effect of the weighting will, by design, be as summarized in Fig. 5, a close-up of a portion of Fig. 2 covering the upper half period of $\mathrm{W}(\boldsymbol{f})$. The response on the other half period follows from the conjugate symmetry of the Fourier transform of a real impulse response.

The third step, evaluation at $x=0$, is represented in (6) by the integral averaging in k of weighted input $\mathrm{W}(\boldsymbol{f})\,\mathrm{L}(\boldsymbol{f})$ over a period in k to produce 1D output spectrum $\mathrm{B}(f)$.

3 DESIGN EXAMPLES

We consider a linear array of 65 elements operating across a bandwidth of $\frac{0.75}{T}$ centered at $f_{\mathrm{RF}}=\frac{3.125}{T}$ before downconversion by an amount $f_{\mathrm{LO}}=\frac{1.625}{T}$ to an IF band centered at $\frac{1.5}{T}$. Element spacing d was set by (5) with $k_{\text{aliasing}}=\frac{0.75}{cT}$, which allows the center of a beam 10° wide at the sidelobes to be scanned to roughly $\approx\pm50^\circ$ from boresight. Figure 6 presents a steerable boresight design and a fixed-direction nonboresight design. Optimization minimized $\alpha\geq 0$ with

$$\frac{1}{\int_{\mathcal{F}_{\text{alias}}} d\boldsymbol{f}}\int_{\mathcal{F}_{\text{alias}}} |\mathrm{W}(\boldsymbol{f})|^2\,d\boldsymbol{f} \leq \alpha^2 \tag{7}$$

$$\frac{1}{\int_{\mathcal{F}_{\text{sl}}} d\boldsymbol{f}}\int_{\mathcal{F}_{\text{sl}}} |\mathrm{W}(\boldsymbol{f})|^2\,d\boldsymbol{f} \leq 10^{-4} \tag{8}$$

and for $k=-K,\ldots,K$,

$$\frac{1}{\int_{\mathcal{F}_{\text{pb}}} df}\int_{\mathcal{F}_{\text{pb}}} \left|\mathrm{W}\left(\left[\begin{smallmatrix}-\sin(\theta_k)(f+f_{\mathrm{LO}})/c\\ f/c\end{smallmatrix}\right]\right)-\beta_k\right|^2 df \leq 10^{-5} \tag{9}$$

with $\beta_0=1$. Sets $\mathcal{F}_{\text{alias}}$ and $\mathcal{F}_{\text{sl}}$ are the 2D aliasing- and sidelobe-supression regions of Fig. 5, and $\mathcal{F}_{\text{pb}}$ is the signal-band interval $\left[\frac{9}{8T},\frac{15}{8T}\right]$. Constraint (7) and the eventual minimization of auxiliary variable α serve together to minimize the mean-square frequency response on the aliasing-suppression region. Constraint (8) bounds the mean-square frequency response on the sidelobe-suppression region. Equation (9) specifies $2K+1$ constraints, with constraint k enforcing response flatness versus f for signals from direction θ_k relative to array normal, this by bounding mean-square error relative to nominal gain β_k, an auxiliary optimization variable that is otherwise unconstrained except for $\beta_0=1$ to fix beam-center gain. Floating these $\{\beta_k\}$ avoids overspecifying main-beam shape. In addition to the above, constraints to enforce linear-phase symmetry $w_{\mathbf{n}}=w_{-\mathbf{n}}$ ensure a real frequency response.

As structured this is a second-order cone program (SOCP) and so can be solved efficiently [5]. The optimization variables comprise coefficients $\{w_{\mathbf{n}}\}$ and the auxiliaries discussed above. When $\boldsymbol{f}$ is fixed $\mathrm{W}(\boldsymbol{f})$ becomes linear in the optimization variables, so the objective is linear in the optimization variables and each constraint is either linear or both quadratic in those variables and a convex function of them.

A filter with 7 coefficents per array element, arrayed in the t direction, and a null-to-null beamwidth of 10° was optimized in the $\theta_0=0$ boresite-beam design, the first in Fig. 6. Specification symmetry ensured $\mathrm{W}(\boldsymbol{f})=\mathrm{W}(-\boldsymbol{f})$, so we reduced problem size with the equivalent $w_{\left[\begin{smallmatrix}n_x\\n_t\end{smallmatrix}\right]}=w_{\left[\begin{smallmatrix}n_x\\-n_t\end{smallmatrix}\right]}$. We constrained the central 8° of the main beam in (9), did not use (8) at all, and replaced $\mathcal{F}_{\text{sl}}$ in (7) with $\mathcal{F}_{\text{sl}}\cup\mathcal{F}_{\text{alias}}$.

There are two ways to point the beam in a different direction. We can use classical time-delay steering using analog or digital time delays at each element. This performs an f-dependent translation in k. Or, we can simply design an off-boresight response as in the second design of Fig. 6, which centers the beam at 30°. That design, which used (7) and (8) as written, increased the number of coefficients per element to 13, without the even symmetry, and yet performance is not dramatically different than for our boresight example. So the system designer must choose between the added complexity of programmable time delays for beam steering or the loss of symmetry and the increased computational, storage, and I/O cost of a library of a directly optimized off-boresight beams.

4 SUMMARY

We have presented a method of digitally sampling a linear antenna array to recover signals over a one-sided bandwidth of up to $\frac{1}{T}$ using A/D conversion at each array element at rate $\frac{1}{T}$, a factor of two improvement relative to conventional Nyquist sampling. This is not paradoxical but is in fact natural, given that the conventional approach leaves empty space in the 2D sampled spectrum when far-field plane waves are sampled. Our factor of two improvement comes partly from recovering that wasted spectral space and partially from a modest increase—a factor between one and two that depends on particulars—in the required element density.

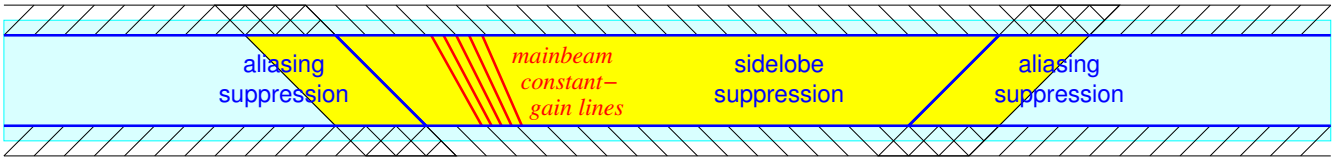

Figure 5: Close up of the $f > 0$ IF-band shaded trapezoid with diagonally hatched filter-transition regions from Fig. 2 superposed over the beam synthesizer's design region, the $f > 0$ shaded box from Fig. 2. Design goals include constant gain in a small mainbeam region, moderate attenuation in sidelobe-suppression regions, and somewhat higher attentuation in aliasing-suppression regions.

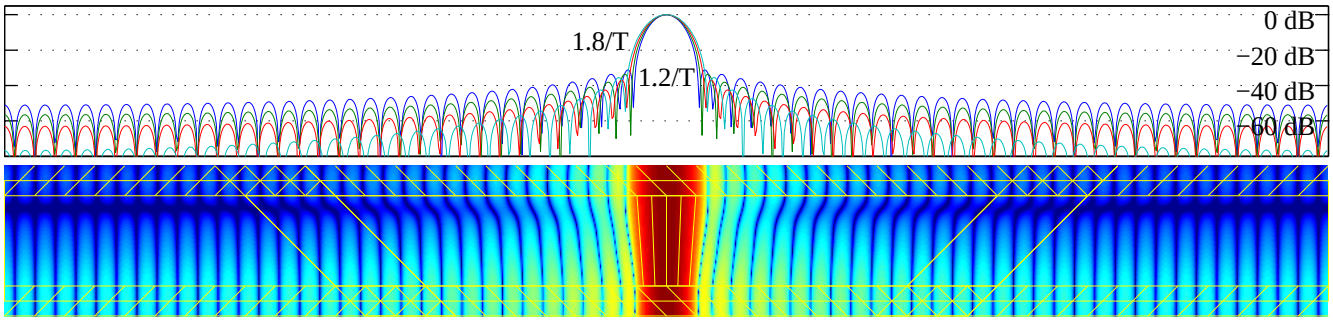

Constant-angle slices (below) of boresight design (above).

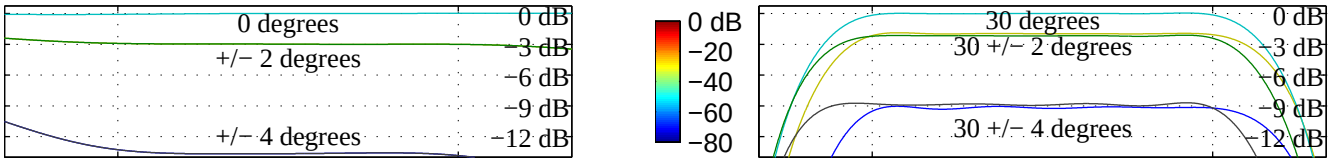

Constant-angle slices (above) of nonboresight design (below).

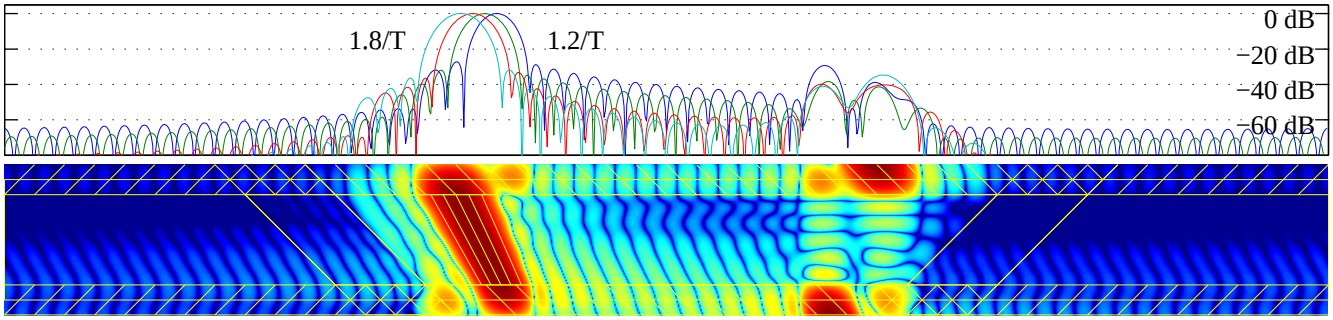

Figure 6: Two example optimized 2D beam-synthesis filter responses for a 65-element linear array. At the top and center left is a boresight design using a 7-tap linear-phase FIR filter at each element (not including beam steering). It has -47 dB RMS gain outside a 10° main beam. At the center right and bottom is a nonsteerable design optimized to center its 10° beam 30° from boresight. It uses a 13-tap nonlinear-phase FIR filter at each element and has -40 dB and -68 dB RMS gains in the sidelobe-suppression and anti-aliasing regions respectively. Responses are shown with slices at five frequencies f and at four main-beam propagation angles.

REFERENCES

[1] J. O. Coleman, "Ping-pong sample times on a linear array halve the Nyquist rate," in *IEEE Int'l Conf. on Speech, Acoustics, and Signal Processing* (http://www.icassp2004.com/), May 2004.

[2] J. O. Coleman and D. P. Scholnik, "Design of nonlinear-phase FIR filters with second-order cone programming," in *IEEE Midwest Symposium on Circuits and Systems* (http://www.mwscas.org/), Aug. 1999.

[3] D. P. Scholnik and J. O. Coleman, "Superdirectivity and SNR constraints in wideband array-pattern design," in *IEEE Int'l Radar Conference* (Atlanta), May 2001.

[4] J. O. Coleman, D. P. Scholnik, and J. J. Brandriss, "A specification language for the optimal design of exotic FIR filters with second-order cone programs," in *The 36th Asilomar Conference on Signals, Systems, and Computers* (http://web.nps.navy.mil/ asilomar), Nov. 2002.

[5] J.F. Sturm, "Using SeDuMi 1.02, a matlab toolbox for optimization over symmetric cones," *Optimization Methods and Software, Special issue on Interior Point Methods (incl. software CD)*, vol. 11-12, pp. 625–653, 1999.